Aquatic Toxicology 174 (2016) 70–81

Contents lists available at ScienceDirect

Aquatic Toxicology

journal homepage: www.elsevier.com/locate/aquatox

Fate of silver nanoparticles in wastewater and immunotoxic effects on rainbow trout

A. Bruneau*, P. Turcotte, M. Pilote, F. Gagné, C. Gagnon*

Aquatic Contaminants Research Division, Environment Canada, 105 McGill Street, Montreal, Quebec H2Y 2E7, Canada

ARTICLE INFO

Article history:
Received 26 June 2015
Received in revised form 18 February 2016
Accepted 18 February 2016
Available online 22 February 2016

Keywords:
Nanotoxicity
Nanoparticle fate
Silver ion
Rainbow trout
Wastewater
Biomarkers

ABSTRACT

Silver nanoparticles (AgNPs) are currently used in technology, medicine and consumer products, even though the fate and the ecotoxicological risks on aquatic organisms of these new materials are not well known. The purpose of this study was to investigate the fate, bioavailability of AgNPs and their effects on fish in presence of municipal effluents. Juvenile rainbow trout were exposed for 96 h to 40 μg/L of AgNPs or 4 μg/L of dissolved silver ($AgNO_3$) in diluted (10%) municipal wastewater. Silver (Ag) concentrations were measured both on water samples and fish tissues (liver and gills). Toxicity was investigated by following immunological parameters in the pronephros (viability, phagocytosis) and biomarkers in liver and gills (cyclooxygenase activity, lipid peroxidation, glutathione-S-transferase, metallothioneins, DNA strand breaks and labile zinc). Results indicated that AgNPs appeared as small non-charged aggregates in wastewaters (11.7 ± 1.4 nm). In gills, the exposure to AgNPs induced morphological modifications without visible nanoparticle bioaccumulation. Dissolved Ag^+ was bioavailable in diluted effluent and induced oxidative stress (lipid peroxidation), labile zinc and a marginal decrease in superoxide dismutase in fish gills. Ag^+ also increased significantly metallothionein levels and inhibited the DNA repair activity in the liver. Finally, the two silver forms were found in liver and induced immunosuppression and inflammation (increase in cyclooxygenase activity). This study demonstrated that both forms of Ag produced harmful effects and AgNPs in wastewater were bioavailable to fish despite of their formation of aggregates.

1. Introduction

Silver nanoparticles (AgNPs) are widely used in technology, medicine and consumer products. They are manufactured for their antimicrobial properties (Dos Santos et al., 2014). Their own properties, with a high surface area ratio, could modify Ag toxicity and class them in a specific contaminant category (NRC, 2012). In a 2010 survey, 1000 consumer products included AgNPs (Massarsky et al., 2014a; Project on Emerging Nanotechnologies, 2013). Although there is a customary use of silver (Ag), the increasing use of AgNPs raises new safety concerns. AgNPs can enter the aquatic environment through washing of treated clothes and the release from products, such as clothes, cosmetics, toothpaste, soaps, and food containers (Benn and Westerhoff, 2008; Ribeiro et al., 2014). Because of their increasing commercial use, legitimate concerns about the release and impacts of AgNPs to aquatic ecosystems are warranted.

Few studies on the behavior of AgNPs in wastewater treatment plants (WWTPs) are found in the literature. Most of AgNPs based consumer products inputs occurs via the release in wastewaters which reaches sewage treated plants (Kaegi et al., 2011). In Germany, intentional or accidental release of nanoscale silver particles Ag-NPs were measured in treated effluent (12 ng/L) for an estimated AgNP load of 4.4 g/day (Siripattanakul-Ratpukdi and Fürhacker, 2014; Li et al., 2013). According to Blaser et al. (2008) Ag residues from Europe, Asia and North America reached 190–410 t/year and between 11.5 to 31.7% of those residues passed through WWTPs and were found in receiving natural water. A significant proportion (about 10%) of the AgNPs which enter in the WWTPs passed through the treatment process and are released by their effluent (Gottschalk et al., 2009; Limbach et al., 2008).

In natural water, AgNPs could be transformed through different processes, such as oxidation, reduction, dissolution, sulfidation, aggregation and adsorption (Lowry et al., 2012). These transformations have an influence on the persistence, mobility and bioavailability of the AgNPs (Lowry et al., 2012). In natural water, the natural organic matter (NOM) could stabilize the nanoparticles (NPs) thus maintaining them in non-aggregated state (Lowry et al., 2012; Cumberland and Lead, 2009). Monovalent Ag^+ could

* Corresponding authors.
E-mail addresses: audrey.bruneau@gmail.com (A. Bruneau), christian.gagnon@ec.gc.ca (C. Gagnon).

http://dx.doi.org/10.1016/j.aquatox.2016.02.013
0166-445X/

bind to organic polyanions, such as fluvic and humic acids (King and Jarvie, 2012). Moreover, the humic substances could also provide long-term reservoir for NPs and maintain them in the column or surface water for over large distance (King and Jarvie, 2012). In wasterwaters, AgNPs are expected to be sulfidized and form Ag_2S in non-aerated system,while in aerated systems they would be unstable with a degradation half-life of days to weeks (Kaegi et al., 2011; Lowry et al., 2012). Kaegi et al. (2011) also found that 10% of metallic Ag (Ag^0) from AgNPs was found in the effluent.

AgNPs were shown to caused cytotoxicity, oxidative stress, damage (lipid peroxidation), reduced mitochondrial activity, and genotoxicity (Gagné et al., 2012; Scown et al., 2010; Braydich-Stolle et al., 2005; Arora et al., 2008; Fabrega et al., 2011; Bruneau et al., 2015). AgNPs can also bind onto cell membranes and affect permeablity and respiratory function of the cells by decreasing the Na^+/K^+ ATPase activity (Morones et al., 2005). The toxicity of AgNPs was partly associated to the release of ionic Ag and NPs induced steric hindrance effects that could lead to protein degradation, DNA damage and lipid peroxidation (Gagné et al., 2013).

The first line of the fishes immune system is the mucus layer found on the surface of the gills, skin and intestines (Jovanović and Palić, 2012). It acts as a barrier shielding the fish from microbial invasion by using lysozyme, lectins, immunoglobulin M (IgM) and other proteolytic enzymes (Bols et al., 2001). This layer can also trap NPs, modify their surface charge properties and decrease their penetration rate (Handy et al., 2008; Jovanović and Palić, 2012). The second line of the immune system of the fish is the pronephros. It is involved in hematopoiesistic i.e., involved in maturation of neutrophils and macrophages and serves as a neutrophil depot (Zapata, 1979). NPs could be internalized in the endolysosomal compartment and engulfed though different processes according to their size. Small NPs (up to 100 nm) are preferentially internalized though calveolae-mediated and clathrin-mediated endocytosis, whereas NPs with a size ≥500 nm are engulfed though receptor mediated phagocytosis or macropinocytosis (Dobrovolskaia and McNeil, 2007; Bartneck et al., 2010; Jovanović and Palić, 2012). Macropinocytosis could be the main uptake route of aggregated NPs (Bartneck et al., 2010). Moreover, the surface charge promotes the engulfment of NPs. Walker and Parsons (2012) demonstrated that NPs with either positive or negative surface charge but less so for neutral NPs activated the phagocytosis activity (Dobrovolskaia et al., 2008; Zahr et al., 2006).

When cells are exposed to AgNPs, reactive oxygen species (ROS) are produced. This process is partly caused by the released ionic Ag form and inflammation process. The ROS such as superoxide anions, hydrogen peroxide and the hydroxyl radical cause oxidative damage, cytotoxicity and DNA damage (Griffitt et al., 2013). During the oxidative burst, the organism's defense mechanism and free metal ligands such as thiols are increased. Also, thiols binding and metallothioneins that are cysteine rich proteins, have been recognised to increase the sequestration of Ag^+ from AgNPs in the liver of trout exposed to surface waters (Gagné et al., 2012).

The purpose of this study was to determine the fate and effects of AgNPs and Ag^+ (as silver nitrate—$AgNO_3$) on rainbow trout, as animal model, after in vivo exposure in diluted wastewater. The Ag concentrations were determined in water and in fish tissues to assess the bioavailability of each silver form. Immunological parameters and biomarkers in liver and gills were performed to evaluate the toxicity of the two Ag forms after an environmental exposure. $AgNO_3$ was chosen to compare the effects of the dissolved form with AgNPs. Dissolved Ag is lethal for aquatic organisms at a concentration of 20 μg/L (Griffitt et al., 2008). A sublethal concentration of dissolved Ag^+ was chosen in this study corresponding approximatively to the labile Ag from the AgNP.

Table 1
Physical characteristics and concentration of total organic carbon (TOC) and dissolved organic carbon (DOC) in the control water utilized for experiments exposure test. The samples were non-exposed to silver.

Control water	TOC (mg/L)	DOC (mg/L)	pH	Conductivity (μS/cm)
Tap water	2.33	2.03	7.45	290
Wastewater	30.3	21.4	7.7	683
10% effluent, T = 0H	7.7	3.44	7.55	273
10% effluent, T = 96H	10.3	8.4	8.45	340

2. Materials and methods

2.1. Silver

A stock solution of PELCO® NanoXact™ AgNPs from Ted Pella Inc (California, USA) was used. According to the manufacturer's specifications, the AgNPs have a mean size of 22 ± 2 nm, are supplied in 2 mM citrate buffer, pH 7.4 and have a zeta potential of −50 mV. For the exposure experiments with AgNPs, a concentration of 40 μg/L total Ag was prepared in 10% of the municipal effluent physically and chemically treated. Silver nitrate ($AgNO_3$) (Sigma–Aldrich, ON, Canada) was dispersed directly in the fish tank at a concentration of 4 μg/L.

2.2. Fish

Juvenile female rainbow trout (*Oncorhynchus mykiss*) (mean head to fork length 121.3 ± 5.5 mm; mean weight 24.3 ± 2.8 g) were provided by a local hatchery (Pisciculture des Arpents-Vert, Ste-Edwidge, Qc), maintained in 1000-L tanks at 15 °C, fed daily with a commercial trout chow during 2 weeks and held under a natural photoperiod (12 h light:12 h dark) prior to exposure experiments.

2.3. Exposure to diluted municipal effluent and silver

A composite wastewater sample was obtained in November 2013 form the Montreal WWTP. The exposure wastewater was diluted 1:10 (v:v) in tap water originating from the St. Lawrence River that was dechlorinated and UV treated (Table 1). Total organic carbon (TOC) and dissolved organic carbon (DOC) concentrations, as well as pH and conductivity were measured at the beginning and the end of the exposure (Table 1). Metal contamination of the Montreal effluent was previously documented by Gagnon et al. (2006) and copper and zinc were the most accumulated metals in caged mussels exposed to the wastewater dispersion plume.

Eight trout were placed in each 20 L containers lined with polyethylene bags and exposed to 10% wastewater with AgNPs (40 μg/L), dissolved silver ($AgNO_3$) (4 μg/L) or without contaminant added. Controls are 10% of effluent water diluted in tap water. The fish were monitored daily for any signs of distress or changes in swimming and breathing behaviour. Dissolved oxygen was maintained above 80%, pH between 7.5–8.6, and temperature at 15 °C during the exposure. The water was not renewed during the experiment. After a 96 h exposure period, the fish were euthanized with 0.1% of MS-222 (Sigma–Aldrich, ON, Canada) using the Canadian Council on Animal Care methods. Pronephros was kept for immune parameter measures. Liver and gills were immediately collected, weighed and stored at −80 °C for subsequent chemical and biochemical analyses.

2.4. AgNP characterization

2.4.1. Transmission electron microscopy (TEM) and electron-dispersive X-ray analysis (EDS)

A sample of AgNPs in 10% wastewater was collected after 96 h and kept at 4 °C. The samples as well as the stock solution were

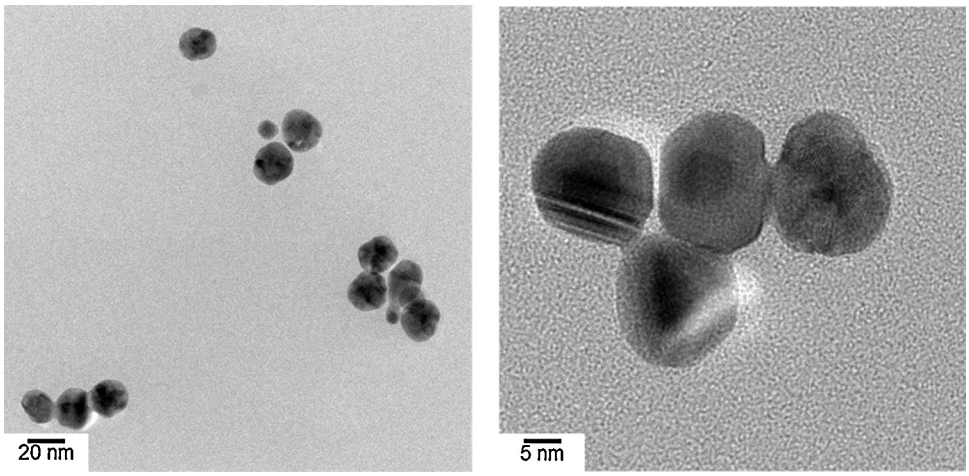

Fig. 1. Transmission electron microscope (TEM) of AgNPs in Ted Pella stock solution. All the nanoparticles were individually separated and present a spherical shape. The scale bars indicate 20 and 5 nm.

observed by TEM no longer than 3 days after the end of exposure. A drop of exposure medium was placed on a copper grid capped with a lacey carbon film for TEM analysis. Once the sample was dehydrated for a few minutes, it was examined by TEM (JEOL, 2100-F model) operated at 200 kV for image capture in clear bottom. For each TEM picture, an electron-dispersive X-ray analysis (EDS) was performed for element composition of targeted particles.

2.4.2. Dynamic light scattering

NPs hydrodynamic size and zeta potential were measured using dynamic light scattering (DLS) (BrookHaven Instrument Corp., ZetaPlus/Bl-PALS) in a stock solution and exposed water. AgNP stock solution was also diluted 1/10 with distilled water before the measurement on the DLS. Each water sample was previously filtered on a 450 nm membrane prior measurements.

2.4.3. Size distribution analysis by filtration and ultrafiltration

AgNPs were characterized for their size distribution by a procedure previously described in Bruneau et al. (2013). Briefly, the AgNPs were fractionated by microfiltration and ultrafiltration using a decreasing membrane porosity size gradient. A subsample of 250 mL of AgNP suspension in each type of water was first filtered on 450 nm hydrophilic PTFE membrane (FHLC04700, Millipore) and 40 mL were then sampled for total Ag determination. The 450 nm filtrate was passed through membranes of three different pore sizes in parallel: 100 nm isopore hydrophilic polycarbonate membrane (VCTP04700, Millipore) and 50 nm mixed cellulose ester membrane (VMWP04700, Millipore) and 25 nm mixed cellulose ester membrane (VSWP04700, Millipore) following by tangential flow ultrafiltration steps.

An ultrafiltration cell with constant agitation was used (Amicon 400 system, Millipore) for the ultrafiltration with 1.5 nm filter size calculated (YM176 mm diameter, 1 kDa cut-off). The pressure in the system was maintained constant at 70 psi, 20 °C, 40 mL, 32 ± 2 min. This ultrafiltration step was considered to provide the "truly" dissolved fraction of Ag. Ag concentrations were evaluated with an ion-coupled plasma mass spectrometry (XSERIES 2 ICP-MS, Thermo Scientific, USA). The operational detection limit is 10 ng/L and the instrumental limit is 3 ng/L. Exposure concentrations were expressed as total Ag in μg/L that was measured in the exposure tanks.

2.5. Silver bioavailability

Livers and gills of fish were individually sampled, weighed and frozen at −80 °C prior to analysis. Tissues were digested with 8 mL of concentrated HNO3 (67–70%), 1 mL of concentrated HCl (32–35%), and 2 mL of concentrated H_2O_2 (30–32%) added in that order. The tissues were then digested during 2 h with a ramp temperature program (maximum 180 °C) using a microwave digestion system (Ethos EZ, Milestone ScientificInc, ON, Canada). Each digested tissue sample was then placed in a 15 mL tube and the final volume was adjusted to 12 mL with deionized water. Total Ag concentration was determined by ion-coupled plasma mass spectrometry (ICP-MS, XSERIES 2 ICP-MS, Thermo Scientific, USA).

2.6. Gills uptake of AgNPs

After 96 h exposure, branchial arcs were dissected out and fixed in a 2.5% glutaraldehyde solution (Electron Microscopy Sciences, PA, USA) in 0.1 M sodium cacodylate buffer (Electron Microscopy Sciences, PA, USA) overnight at 4 °C. Those samples were washed three times with 0.1 M sodium cacodylate washing buffer (Electron Microscopy Sciences, PA, USA) for 1 h. Samples were then post-fixed in 1% of osmium tetroxide solution (Mecalab, QC, Canada) with 1.5% aqueous potassium ferrocyanide for 2 h. Then the samples were washed 3 times with the washing buffer for 15 min. Cells were dehydrated in increasing concentration of acetone (Fisher Scientific): 30%, 50%, 70%, 80%, 90%, and three times at 100% each for 8–15 min. Then the samples were infiltrated with Epon (Mecalab, QC, Canada)/acetone mix. Samples were embedded with appropriate labels then polymerized in a 60 °C oven for 48 h. Transversal cut were made in the branchial filaments. Sections were trimmed and cut at 90–100 nm thick sections with UltraCut E ultramicrotome (Reichert-Jung, NY, USA) laying onto a 200 mesh copper grid (Electron Microscopy Sciences, PA, USA). Finally, sections were stained with uranyl acetate (Electron Microscopy Sciences, PA, USA) for 8 min, then Reynold's lead (Electron Microscopy Sciences, PA, USA) for 5 min. The sections were analyzed with FEI Tecnai 12 120 kV transmission electron microscope (TEM) equipped with an AMT XR80C 8 megapixel CCD camera. For electron-dispersive X-ray analysis, sections with the same thickness were placed onto a carbon-coated grid. EDS were performed on the picture with a Philips CM200 200 kV TEM equipped with Gatan Ultrascan 1000 2k x 2k CCD Camera System Model 895 and EDAX Genesis EDS.

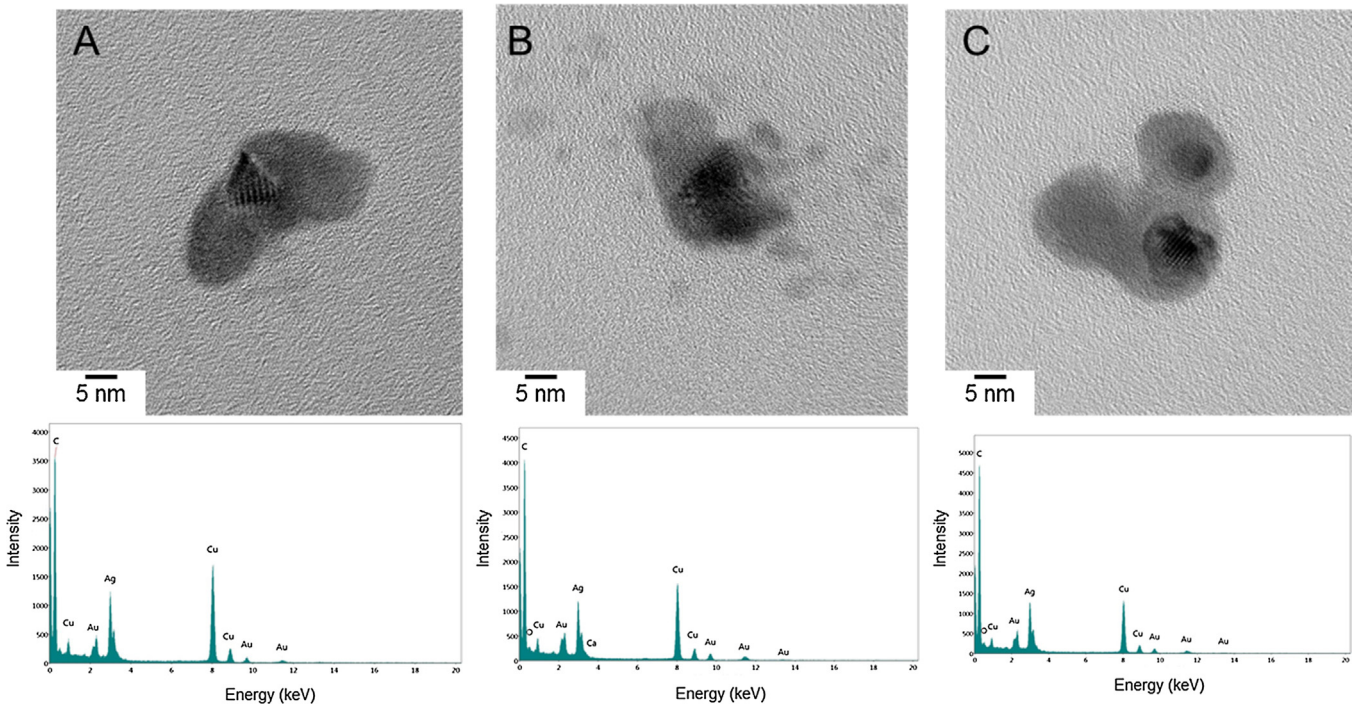

Fig. 2. Silver morphology in wastewater after 96 h exposure and elemental composition analysis. Ag nanoparticles were retrieved in small aggregates. The energy dispersive spectra (EDS) elemental analysis data are presented below for each images confirm that each image show silver nanoparticles. The scale bars indicate 5 nm.

2.7. Immune parameters

Immune parameters were performed in fish leucocytes according to an adapted method from Brousseau et al. (1998). Briefly, leucocytes extracted from the pronephros were then collected by centrifugation of a 51% Percoll gradient (Sigma–Aldrich, ON, Canada) at 400 g, 30 min, 20 °C. After washing steps the ratio of live to dead cells was assessed using trypan blue dye exclusion under a microscope with a hemocytometer and it exceeded 90%.

Viability of immune cells was performed according to an adapted method from Brousseau et al. (1998). Cells at a concentration of 2 million/mL were incubated in dark light over 18 h at 15 °C in duplicate. Following the incubation, the cells were washed and resuspended in Roswell Park Media Institute (RPMI) containing 10% FBS, 100 U/mL penicillin, 100 μg/mL streptomycin and 10 mM HEPES. Viability was observed by flow cytometry using propidium iodide (PI; Sigma–Aldrich, ON, Canada). PI fluorescence for each sample was measured in duplicate with a flow cytometer equipped with an argon laser excitation ($\lambda = 488 \pm 10$ nm) (Guava Easycyte, Millipore, USA) at 625 ± 42 nm, and 5000 events were registered.

Phagocytic activity for macrophages was measured following the protocol of Brousseau et al. (1998). Briefly, 1 mL of adjusted cell concentration (2 million/mL) was added to 24 cell cultures coated well plate in duplicate. Cells were incubated with a ratio 100:1 of fluorescent latex beads (Polysciences, PA, USA) in order to observe the phagocytosis capacity of the cells. After an incubation period of 18 h at 15 °C, the cell suspensions were overlaid with a gradient and fixed in 0.5% formaldehyde and 0.2% sodium azide in a PBS solution (Sigma–Aldrich, On, Canada). Latex bead fluorescence was measured with a Guava Easycyte (Millipore, USA) in duplicate at $530 \text{ nm} \pm 42$ nm bandwidth, and at least 10,000 events were registered. The immunoactivity was defined as the number of cells containing one or more beads and the immunoefficiency as the number of cells that containing three beads or more.

2.8. Biochemical biomarkers

Frozen liver and gills were homogenized according using a Teflon pestle tissue grinder during 20 s in ice-cold homogenization buffer (10 mM Hepes-NaOH, pH 7.4 containing 140 mM NaCl, 1 mM dithiothreitol and 1 mg/mL aprotinin). Aliquots of samples were taken for lipid peroxidation (LPO), DNA strand breaks, and total proteins determinations. Another part of the homogenate was centrifuged at $15{,}000 \times g$ for 20 min at 4 °C (S15). The supernatant of each sample was taken for labile zinc (labile Zn), metallothioneins (MT), activity of cyclooxygenase (COX), glutathione S-transferase, superoxide dismutase (SOD), and proteins determinations.

LPO was determined according to the thiobarbituric acid (TBARS) methodology using microplate assay (Wills, 1987; Gagné, 2014). Thiobarbituric acid reactants were detected by fluorescence at 540 nm excitation and 590 nm emission. The data were expressed as g TBARS/mg proteins. DNA strand breaks were determined using the alkaline precipitation of Olive (1988) with fluorescent-based DNA strands detection. DNA strands were detected using the Hoechst dye at 360 nm excitation and 460 nm emission (Synergy 4, BioTek, USA). DNA quantification was measured with standard solutions of Salmon sperm DNA. The data were expressed as ug DNA/mg of proteins.

Levels of labile Zn were detected in the S15 fraction by a fluorescence probe methodology (Gagné and Blaise, 1996). Fluorescence reading were taken at 360 nm excitation and 460 nm emission in a microplate reader (Synergy 4, BioTek, USA) and calibrated with standard solutions of zinc sulfate. Data were expressed as ng zinc equivalents/mg proteins. Glutathione S-transferase (GST) was determined a spectrophotometric methodology using 2,4-dichloronitrobenzene as the co-substrate and reduced GSH as described elsewhere (Gagné, 2014). The data were expressed as the increase in absorbance at 340 nm/min/total proteins. The activity of superoxide dismutase (SOD) was determined using a chemical superoxide anion generator (Ewing and Janero, 1995). The principle of the assay consists of the ability of SOD to prevent the

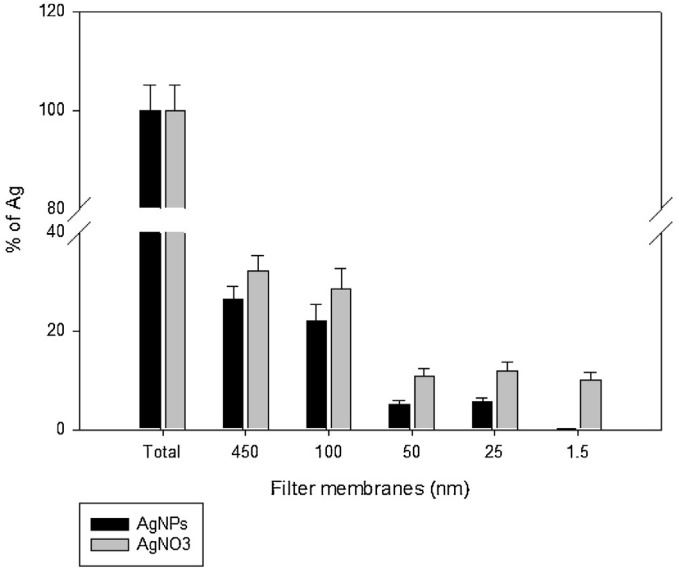

Fig. 3. Percentage of Ag in water after 96 h exposure. The total Ag concentration after 96 h were 25.7 μg/L and 3.75 μg/L for AgNPs and $AgNO_3$ respectively. Total corresponds to the non-filtered fraction, 450 nm, 100 nm, 50 nm, and 25 nm stands for filtered fractions; 1 kDa corresponds to the truly dissolved fraction (Ag^+).

reduction of the colorimetric dye *p*-iodonitrotetrazolium in the presence of an equimolar mixture of phenazine methosulfate and reduced NADH (superoxide generator). The data were expressed as absorbance units/min/mg proteins. The activity of cyclooxygenase (COX) in hepatocytes was measured according to the protocol of Gagné (2014). The activity of the COX increases the oxidation of the arachidonic acid and produced cycloendoperoxide. The assay measures the elimination of cycloendoperoxide by peroxidase and dichlorofluorescein substrate. Fluorescence readings were taken every 5 min according to a kinetic from 0 to 30 min, at 485 nm for excitation and 535 nm for emission (Synergy 4, BioTek, USA). The data were expressed as ΔRFU (increase of the relative units of fluorescence)/(min × mg proteins).

All the biomarkers were normalized with the total individual protein concentration according to Bradford methodology (Bradford, 1976) with bovine serum albumin for calibration. Total protein concentration was measured at 595 nm by a microplate reader (PowerWave, BioTek) in duplicates.

Total level of metallothioneins (MT) was determined using a Ag saturation assay adapted from Scheuhammer and Cherian (1986). The method consists in the saturation of MT with an excess of Ag and this excess is removed with haemoglobin. A 50 μL sample of the S15 was mixed was mixed with 50 μL of 10 ppm Ag^+ in 0.2 M glycine-NaOH, pH 8.5. The blank composed by 50 μL of homogenisation buffer. A positive control composed by a standard of 20 ng MT (Enzo Life Sciences, Inc., NY, USA) in Tris HCl 25 mM, 0.1 DTT pH 6.4 was also added. After 10 min incubation, 400 μL of glycine–NaOH buffer was added and 50 μL of haemoglobin 2% was added and incubated during 5 min. The samples were heated for 2 min at 100 °C and centrifuged at 10,000 × *g* for 5 min to precipitate Hb and other proteins. The last step was repeated on more time. The supernatant was analysed in triplicate diluted 1/10 in water by graphite furnace-atomic absorption (GF-AAS) equipped with Zeeman background correction (240Z AA with Zeeman GFAA, Agilent). Each sample absorbance was calculated according to an Ag^+ calibration curve (0–15 μg/L). The equivalent MT concentration in liver was estimated with the standard MT and data were normalized with the total individual protein concentration (μg MT equivalent/mg proteins).

Table 2
Mean size and zeta potential of AgNPs in stock solution and 10% effluent. These results were observed with a DLS after filtration through a membrane of 0.45 μm in order to eliminate large aggregates in the solution and measure the mean diameter size of the particles.

Samples	Mean diameter size (nm)	Zeta potential (mV)
Stock solution	19.2 ± 0.3	−58.02 ± 4.21
10% effluent	11.7 ± 2.1	0.00 ± 0.00

2.9. Data analysis

The normality of the data distribution was verified with Kolmogorov–Smirnov' test. Differences between control and exposed treatments were examined using paired *t*-test when data normality was confirmed. Data were log-transformed when significant deviation from normality occurred and Kruskal Wallis ANOVA was used. Significance was set at $p < 0.05$.

Pearson-moment correlations were performed for studying the relation among biochemical results for both Ag forms. Discriminant analysis was performed to examine the global response patterns of the 9 biomarkers and bioaccumulation data (bioaccumulation, immunoactivity, immunoefficiency, COX activity, GST activity, LPO, SOD, genotoxicity, labile Zn, and MT) between the control and the exposed groups. All the statistical analyses were conducted with STATISTICA (version 7, StatsoftInc., 1995).

3. Results

3.1. Characterization of AgNPs in 10% effluent

After 96 h exposure, TOC was increased from 7.7 to 10.3 mg/L (+34%) and DOC was increased from 3.44 to 8.4 mg/L (+41%) (Table 1). These results reflect the release of excrements from fish during the experiment. pH values were also increased (from 7.45 to 8.5).

AgNPs in stock solution had an initial mean diameter of 20 nm (Fig. 1) as shown by TEM image analysis, which corresponds to the manufacturer's information. They had a spherical shape and were mainly in monomeric form. Once in diluted wastewater, TEM image analysis revealed that wastewater induced changes in the NPs size and form (Fig. 2). Small aggregates of 3–4 NPs were observed (Fig. 2). The EDS graphs 1–3 confirm that all the observed NPs were AgNPs (Fig. 2). AgNPs maintained their originated spherical form (Fig. 2A and B), but morphological transformations were also observed (Fig. 2B) confirming that AgNPs could lose their original shape in diluted effluent in tap water. On one hand, breakdown was detected (Fig. 2B) in diluted effluent where AgNPs of 20 nm diameter were observed with other small NPs surrounding them. On the other hand, aggregation phenomenon seen in Fig. 2C suggests aggregation of the AgNPs involving with the capping layer. The EDS graphs 1–3 confirm that all the observed NPs were AgNPs (Fig. 2).

The mean diameter of AgNPs measured by DLS in stock water was under the manufacturer's specifications (Table 2). In the wastewater, the mean size of AgNPs was about 12 nm, corresponding to "degraded" small particles (or NP fragments). Difference between the TEM observations and DLS measurements would be due to the filtration step (on 450 nm membrane) as a pre-treatment procedure prior to DLS measurements. The filtration step was performed prior DLS measures to remove aggregates and increase the accuracy of the result. The zeta potential of zero could be due to the neutralization of the total charge of the NPs in diluted effluent.

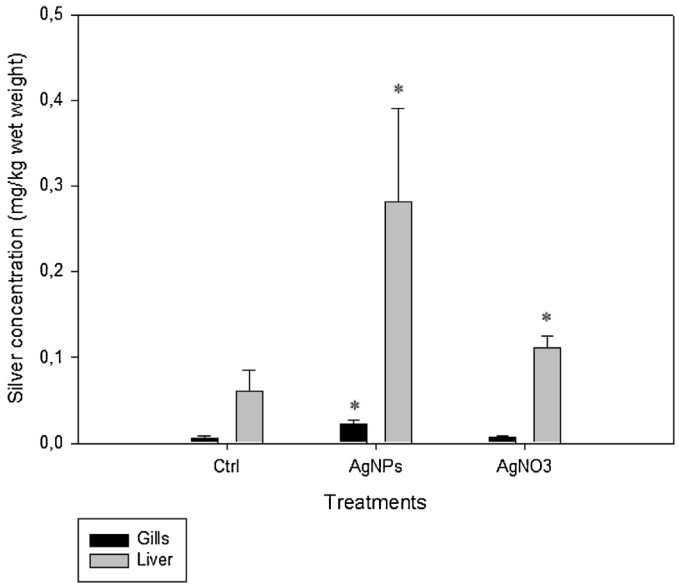

Fig. 4. Ag concentrations (mg/kg wet weight) in gills and livers of rainbow trout exposed 96 h to AgNPs and $AgNO_3$. Fish were initially exposed to 40 μg/L of AgNPs and 4 μg/L of $AgNO_3$. Error bars correspond to standard error. Stars indicate significant differences between silver treatments and control ($p < 0.05$).

3.2. Silver size distribution in diluted wastewater

After a filtration step on 450 nm, only 26% of Ag from AgNPs and 32% of Ag from $AgNO_3$ were detected in diluted wastewater, indicating that circa 75% of Ag was preferentially linked to particles ≥450 nm (Fig. 3). Interestingly, 5.5% (1.4 μg/L) of the AgNPs passed throughout the 25 nm filter, confirming that only a small percentage of the AgNPs remained in the original monomeric form. No AG was detected in 1 kDa or less. Ag from the $AgNO_3$ was found in the filtered 25 nm fraction (0.44 μg/L = 12%), but most of it 10% (0.37 μg/L) was found in the truly dissolved (1 kDa) fraction (Fig. 3), suggesting that only 10% of Ag from $AgNO_3$ was considered truly dissolved.

3.3. Silver in fish tissues

A significant increase in Ag concentration was measured in gills and livers of fish exposed to AgNPs (Fig. 4). The liver accumulated more Ag than gills which suggest a systemic distribution of AgNPs in fish. A significant bioaccumulation of Ag was observed with with $AgNO_3$ solution in liver (0.11 mg/kg wet weight of Ag) but was not significantly detected in gills (0.007 mg/kg wet weight of Ag).

TEM pictures of gills fish controls (Fig. 5A–C) show chloride cells with some mitochondria. We found no AgNPs in the gills filaments. EDS were performed on the pictures and did not indicate Ag accumulation suggesting the absence of colloidal Ag in fish gills exposed to diluted effluent. However, exposed gills (Fig. 5D–F) showed cellular damage such as enlarged vacuoles, increased mitochondria number, and compaction of the reticulum although no AgNPs were detected. Moreover, inclusion bodies were also observed indicating an effect of the AgNPs on the gills structure.

3.4. Immunocompetence evaluation

No decrease in lymphocytes and macrophage viability was observed after an exposure to AgNPs. Only one significant decrease was observed for macrophage viability between control and $AgNO_3$ treatment ($p < 0.05$).

Significant decreases in immunoactivity and immunoefficiency were observed between the control and $AgNO_3$ treatment (Fig. 5). With AgNPs, a significant decrease in immunoefficiency between the control (diluted effluent alone) and the exposed samples was observed. These results indicate that AgNPs have an immunosuppressive effect without affecting the viability of the cells (Fig. 6).

3.5. Biomarkers of toxic stress

In gills, a significant increase in labile Zn with both Ag forms was observed (Fig. 7) suggesting the released of Ag^+ from AgNPs and $AgNO_3$ in gills tissue. Labile Zn was also significantly correlated with gills Ag levels ($r = 0.40$, $p < 0.05$) (Table 3). LPO was non-significantly increased with $AgNO_3$ in fish gills (Fig. 7). The increase in LPO was negatively correlated with the immune parameter (immunoactivity: $r = -0.52$, $p < 0.05$; immunoefficiency: $r = -0.42$, $p < 0.05$). Although SOD was not significantly induced, the activity was negatively correlated with LPO which suggests that decreased SOD was involved in LPO in gills in part at least. Significant increases in GST were observed with AgNPs and $AgNO_3$. No significant variation in DNA strand breaks were observed with AgNPs and $AgNO_3$. GST was significantly correlated to SOD ($r = 0.46$, $p < 0.05$) and DNA strand breaks ($r = 0.77$, $p < 0.05$) indicating that gill biochemical effects were partly associated with oxidative stress and membrane damage due to direct contact with both Ag forms.

In liver, significant increase in cyclooxygenase activity was observed with the two forms of Ag, indicating an inflammation which was correlated with the decrease in phagocytosis activity ($r = -0.43$, $p < 0.05$), and in phagocytosis efficiency ($r = -0.44$, $p < 0.05$) (Table 3). In the liver, COX activity was also correlated with labile Zn ($r = -0.41$, $p < 0.05$), MT level ($r = 0.41$, $p < 0.05$), and Ag tissue levels ($r = 0.55$, $p < 0.05$) (Table 3). Significant decreases in labile Zn were observed in liver oxidative activity in cells (Fig. 7). In the liver, the DNA strand breaks was negatively correlated with the LPO ($r = -0.46$, $p < 0.05$), suggesting that modifications in the DNA repair process is linked to the increase of the LPO. An inhibition in the DNA repair activity was suggested in the liver, because a significant decrease in DNA strand breaks was observed with $AgNO_3$ and not with AgNPs (Fig. 7). The MT level was also correlated to the GST activity ($r = 0.81$, $p < 0.05$) (Table 3). A significant increase in MT levels with $AgNO_3$ was observed, confirming the involvment of MT in Ag exposure and toxicity the (Fig. 7). The increase in MT level was not observed with AgNPs suggesting that no important release of Ag^+ occurred during the time of exposure (Fig. 7).

The treatments were well separated according to the discriminante fonction (DA). According to Wilks' lambda, the 2 axis were significant ($F(22.94) = 5.1665$ $p < 0.001$) where 30% of the variance was explained by axis x and 23% of the variance were explained by axis y. The effects of AgNPs were well separated by the x axis where phagocytic activity and efficiency were the main biomarkers that discriminated the biochemical response of exposed from non exposed fish while GST and SOD were the main biomarkers that discriminated $AgNO_3$ from AgNPs treatments. DA confirmed that forms of Ag differed in the presence of diluted wastewater (Fig. 8); oxidative and anti-oxidative pathways were involved with $AgNO_3$ treatment while inflammation and immune pathways were involved with the AgNP treatment.

4. Discussion

4.1. Silver speciation

This study investigated the fate, bioavailability and toxicity of dissolved Ag and AgNPs in the presence of diluted wastewater. The study revealed that 75% of the original concentration of Ag as

Table 3
Pearson correlations calculated between 9 biomarkers (COX = cyclooxygenase, GST = glutathione S-transferase, SOD = superoxide dismutase, DNA = DNA strand breaks, lab Zn = labile zinc, LPO = lipid peroxidation, MT = metallothioneins, Phago activity = immunoactivity, Phago efficiency = immunoefficiency) and Ag bioaccumulation data (Bio liver = bioaccumulation in liver and Bio gills = bioaccumulation in gills) from all the data of AgNPs and $AgNO_3$.

	COX liver	GST liver	SOD liver	DNA liver	Lab Zn liver	LPO liver	Bio liver	MT liver	GST gills	SOD gills	DNA gills	Lab Zn gills	LPO gills	Bio gills	Phago activity	Phago efficiency
COX liver	1.00															
GST liver	0.36	1.00														
SOD liver	0.07	0.28	1.00													
DNA liver	−0.35	−0.17	−0.10	1.00												
Lab Zn liver	−0.41*	0.34	0.14	0.02	1.00											
LPO liver	0.12	0.28	−0.11	−0.46*	0.12	1.00										
Bio liver	0.55*	−0.07	0.09	0.01	−0.35	−0.25	1.00									
MT liver	0.41*	0.81*	0.26	−0.20	0.25	0.18	0.03	1.00								
GST gills	0.44*	0.16	−0.05	0.33	−0.09	−0.46*	0.54*	0.01	1.00							
SOD gills	−0.14	−0.17	0.28	0.25	0.11	−0.51*	0.55*	−0.15	0.46*	1.00						
DNA gills	0.32	0.42*	−0.10	0.04	0.32	−0.19	0.32	0.28	0.77*	0.34	1.00					
Lab Zn gills	0.41*	−0.01	0.19	−0.11	−0.23	−0.13	0.47*	0.05	0.29	0.32	0.02	1.00				
LPO gills	0.30	−0.15	−0.11	−0.26	−0.53*	0.16	−0.14	−0.25	−0.07	−0.48*	−0.20	0.14	1.00			
Bio gills	0.31	−0.20	0.14	−0.08	−0.36	−0.16	0.86*	−0.05	0.18	0.52*	0.00	0.40*	−0.19	1.00		
Phago activity	−0.43*	−0.28	−0.19	0.26	0.31	−0.26	0.15	−0.28	−0.02	0.30	0.08	−0.23	−0.52*	0.23	1.00	
Phago efficiency	−0.44*	−0.17	−0.06	0.39*	0.36	−0.33	−0.05	−0.30	0.08	0.25	0.10	−0.21	−0.42*	−0.06	0.89*	1.00

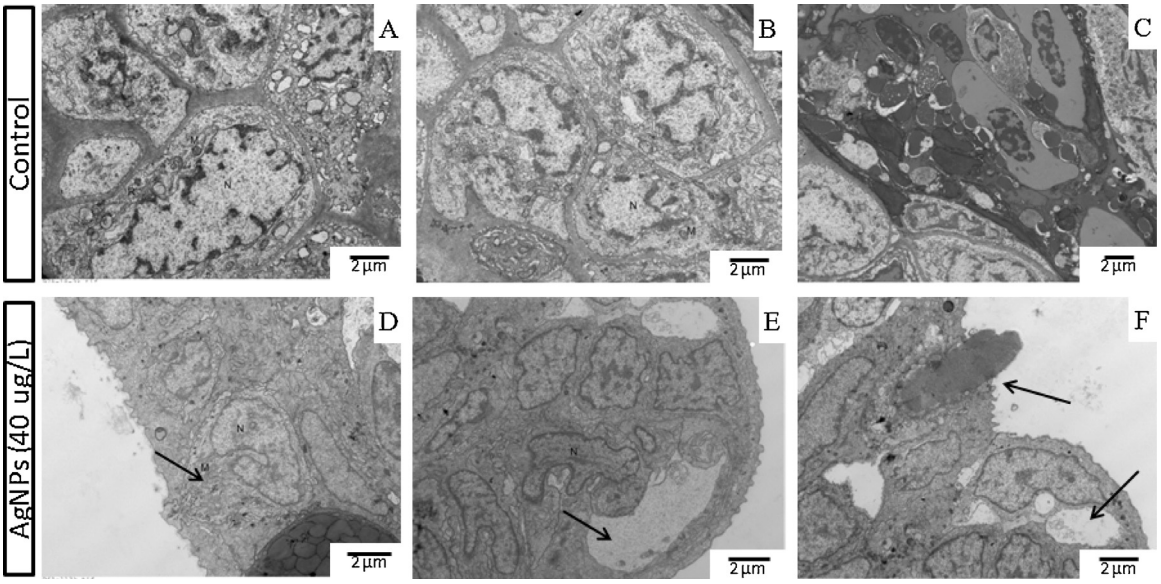

Fig. 5. TEM imagery of gills of non-exposed (A–C) and exposed fish (D–F) to AgNPs for 96 h. M = mitochondria, N = nucleus. Arrows indicated morphological gills modifications. No significant accumulation of AgNPs was observed in gills, but structural changes were observed, such as: mitochondria number increase (D), nucleus invagination (E) and compaction of the reticulum (E) and vacuoles (E and F). All the pictures were made with ×2900 magnification and 120 KeV. The scale bars indicate 2 µm.

AgNPs or $AgNO_3$ was retrieved as large colloids (>450 nm). However, AgNPs were also retrieved in the 25 nm filtered fraction. It is noteworthy that some AgNPs also lost their original shape showing degradation in wastewaters. In other studies, dissolved organic matter (DOM) interacts with AgNPs coating and induced their surface charge neutralisation hence dissolution (Unrine et al., 2012; Philippe and Schaumann, 2014). In our study, no Ag^+ was measured in the truly dissolved fraction (1.5 nm), which suggests that toxicity must have proceeded by different means rather than Ag^+ mediated effects. This was further supported by the lack of MT induction in the liver of fish exposed to AgNPs albeit labile Zn levels were increased. A previous study showed that a fraction of added AgNPs (1–2%) was dissolved at a pH 6 to 9 after an 24 h *in vivo* exposure of bacterial strain (Siripattanakul-Ratpukdi and Fürhacker, 2014; Fabrega et al., 2009). This was in the same range of our data where in the order of 5% of added Ag was found at the 25 nm filtrate (Fig. 3). Osborne et al. (2013), also demonstrated that AgNPs slowly released Ag^+ (0.1–2%) during exposure which accounts for the antimicrobial function of AgNPs. Thus, a small part of the AgNPs can be expected to dissolve in the media depending on the pH, conductivity and NOM. As observed in our TEM pictures these small fractions would be still in monomeric form in diluted wastewaters, whereas in surface or tap water, AgNPs took a chain and star shape appearance after 96 h exposure (Bruneau et al., 2015).

The neutral zeta potential of the AgNPs and the TEM results suggest that NPs were aggregated and their surface charge was neutralized by the DOM as it was observed by Unrine et al. (2012). As observed in Bruneau et al. (2015) natural water neutralized the surface charge of AgNPs 20 nm after 96 h in vivo exposure with rainbow trout. Moreover the AgNPs were retrieved in aggregates after 96 h exposure as it was observed in this study (Bruneau et al., 2015).

The increase in DOC and conductivity could have prevented a more completed dissolution of the monomeric AgNPs in Ag <1 kDa. Past studies showed that NOM could bind metal and will reduce the toxicity of metal to aquatic organisms (Welsh et al., 1993). Erickson et al. (1998) also provided evidence of pH effect on Ag complexation

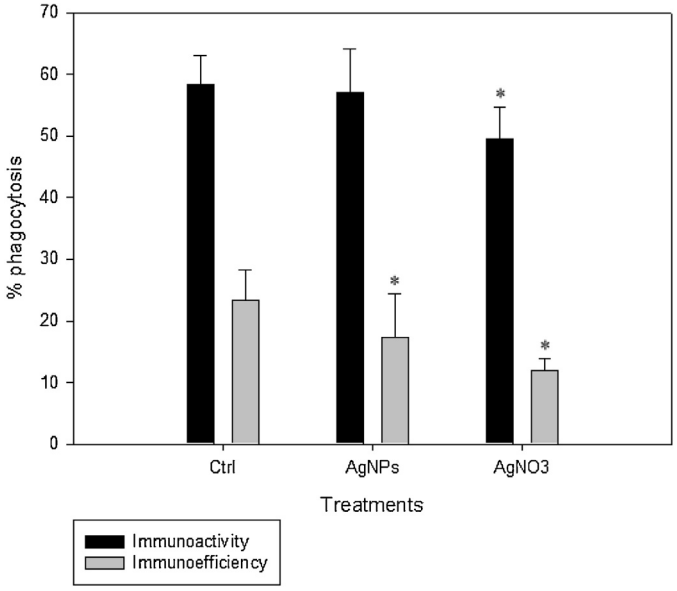

Fig. 6. Immunoactivity (phagocytosis of 1 bead and more) and immunoefficiency (phagocytosis of 3 beads and more) of rainbow trout exposed to AgNPs and $AgNO_3$ for 96 h. Error bars correspond to standard error. Stars indicate significant differences between silver treatments and control ($p < 0.05$).

capacity of DOC. The potential for Ag^+ to be bound to DOC molecules decreases with the increase in H^+ concentration. In our case, the alkaline pH of the media increases the amount of Ag^+ that DOC can bind and could explain the formation of small NPs observed in TEM and the low percentage of ionic form in the water.

In this study, $AgNO_3$ was bioavailable as small fractions (0.5 μg/L in the 25 nm pore size membrane), and as Ag^+ because a small amount (0.4 μg/L) of the initial Ag concentration was still bioavailable in the truly dissolved fraction or permeate fraction. Ag^+ which are retrieved in the permeate fraction of 1 kDa is likely assimilated by the fish. Although both forms of Ag readily formed large aggregates including Ag_2S, AgNPs also occurred as small aggregates (25–450 nm) and were absent from the truly dissolved fraction of Ag (<1 kDa). This result indicates that both Ag forms have different fate in the same diluted wastewater but were still bioavailable.

4.2. Silver uptake

AgNPs enter in the organism as monomeric NPs without apparent build-up accumulation at the surface and in the gills, suggesting a weak bioconcentration in this tissue. Other uptake pathways may also be suggested such as the gastro-intestinal entrance (Scown et al., 2010). Moreover water parameters such as conductivity, pH and NOM could reduce the Ag bioaccumulation; Bury and McGeer Wood (1999) have previously demonstrated that Ag bioaccumulation could be reduced with the increase in DOC. Our results are not in agreement with those of Scown et al. (2010), who observed AgNP inclusion in brown trout gills with low tissue damage. Farkas et al. (2011) also observed AgNPs accumulation around the nucleus of gills cells. In other studies, Ag were retrieved in both zebrafish (Griffitt et al., 2009) and perch gills (Bilberg et al., 2010) at much higher Ag concentrations (0.3–1 mg/L) than in the present study. Not withstanding this, there was some gills damage in this study-trivial. Our histological results showed gill tissues with vacuoles that were in agreement with the results of Farmen et al. (2012) who observed a lifting of the secondary lamellae from the gills basement layer after an exposure to 100 μg/L AgNPs. We also observed an increase in the mitochondria number, and a compaction of the reticulum, indicating an impairment of the gills function and maybe an impairment of the osmoregulation caused by the contact with AgNPs.

Our data showed that AgNPs were principally assimilated through ingestion of water. This is consistent with the increased presence of AgNPs aggregates and Ag hepatic levels. This is agreement with the observation that fish absorbs about 30% of their body mass as water per day during drinking and eating, which could significantly contribute to the Ag uptake. Based on the liver Ag content data, a bioconcentration factor (BCF) of 11.5 and 26.5 were calculated for AgNPs and $AgNO_3$ respectively suggesting that Ag aggregates in diluted effluent from $AgNO_3$ were 2.3 times more bioavailable than Ag aggregates from AgNPs in the same media. In this study, total Ag concentration in liver for AgNP exposure was 0.3 mg/kg and in exposure media the total Ag concentration was 26 μg/L after 96 h. Ours results are similar to those of Scown et al. (2010), who observed significant accumulation of AgNPs (100 μg/L) of 10 nm and 35 nm diameter after a 10 days exposure in fish liver; Ag concentrations ranged from 0.3 to 0.6 mg/kg and from 1 to 1.6 mg/kg in gills and in liver respectively. For $AgNO_3$ treatment, the liver bioaccumulation reached an average of 0.1 mg/kg and in exposure media the total Ag concentration in $AgNO_3$ was 3.75 μg/L; these results indicated a BCF with Ag^+ which is higher than that observed with AgNPs. Dissolved Ag was likely more easily absorbed and concentrated in fish than were AgNPs by these organisms. Thus, wastewater would promote the absorption rate of the dissolved Ag form. Our bioaccumulation results was also in agreement with those of Gomes (2014) who observed a significant increase in Ag concentrations in digestive gland of mussel after 3 days of exposure with $AgNO_3$ and AgNPs. These authors also demonstrated that the accumulation of Ag from AgNPs occurs either by dissolved AgNP and AgNPs uptake.

4.3. Toxic effects

According to our results, the bioaccumulated AgNPs and $AgNO_3$ induced toxic effects. On the one hand, $AgNO_3$ increased the LPO and its correlation with labile Zn, confirm the harmful effects of direct contact between Ag^+ and the gills. Also the marginal decrease in SOD activity indicates a loss of the oxidative stress control in this tissue. Ag^+ also induced significantly MT levels and induced damage to DNA. The decrease in DNA strand breaks suggest an inhibition of DNA repair activity that was previously observed in fresh water mussel exposed to quantum dots (Gagné et al., 2008).

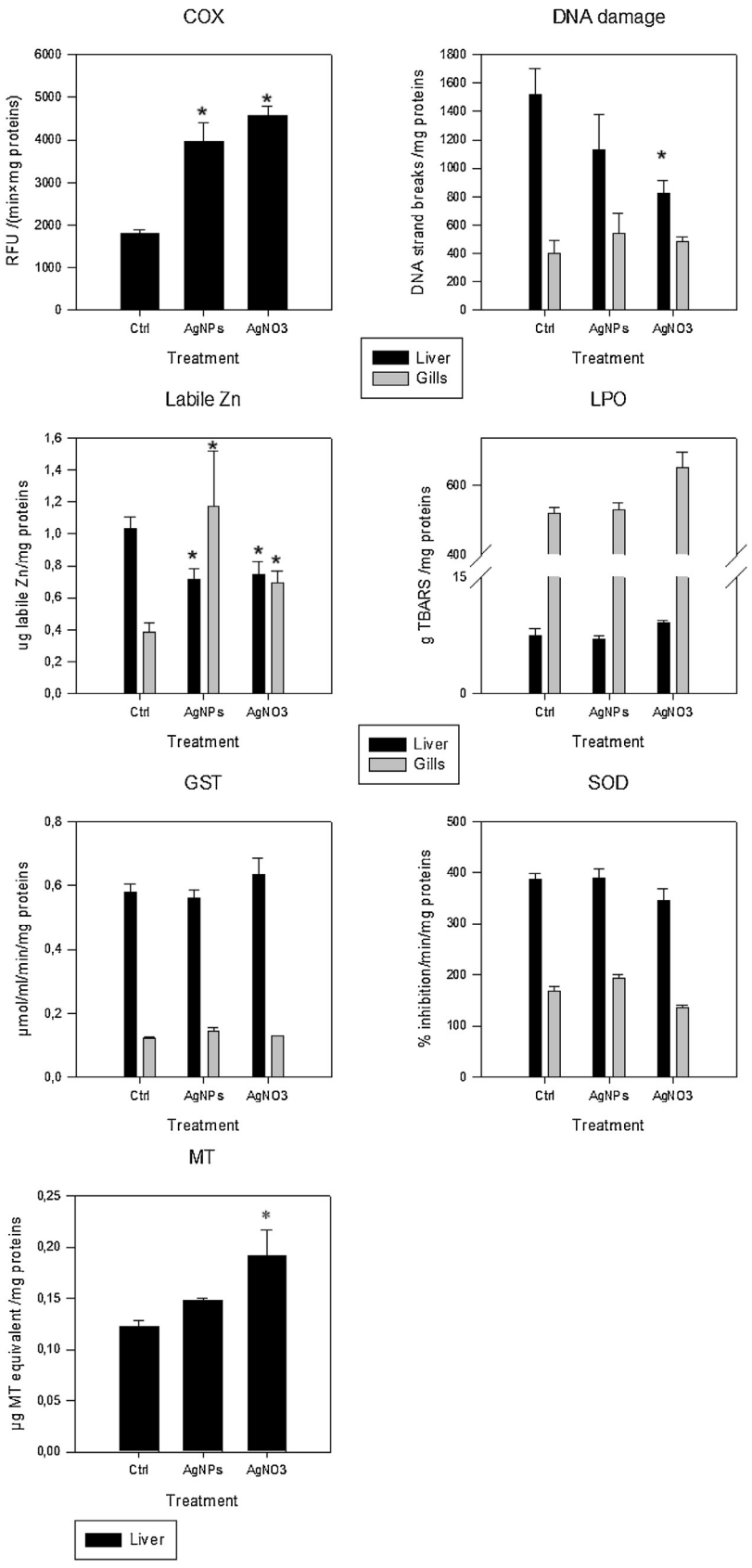

Fig. 7. Biomarkers in gills and liver of fish exposed to AgNPs and $AgNO_3$ for 96 h. COX = cyclooxygenase activity, DNA damage, Labile Zn = labile linc, LPO = lipid peroxidation, GST = glutathione S-transferase activity, SOD = superoxide dismutase, and MT = metallothionein level. Error bars correspond to standard error, stars indicate significant differences between silver treatments and control ($p < 0.05$).

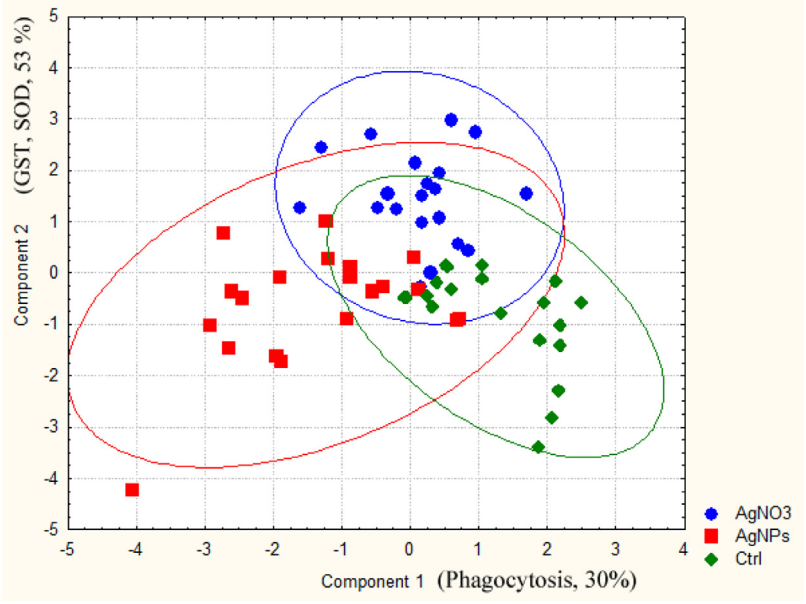

Fig. 8. Discriminant analysis between all the results and treatments. No association between treatments was observed. Phagocytic activity and efficiency were the main biomarkers that discriminated the biochemical response of exposed from non-exposed fish and explained 30% of the data variance (component 1). Glutathione S-transferase (GST) and superoxide dismutase (SOD) were the main biomarkers that discriminated the $AgNO_3$ from AgNPs treatments and explain a cumulated percentage of 53% of variance (component 2). Ellipses correspond to the confidence interval around all the data for all the treatment. Confidence intervals are fixed at 95%. According to the figure, there is some degree of similarity of Ag and AgNPs. AgNPs differs from $AgNO_3$ from the *x* axis i.e., phagocytosis.

Finally, Ag^+ induced immunosuppression and leucocytes cytotoxicity. On the other hand, with AgNPs a small increase in labile zinc in gills indicated that AgNPs could release Ag^+ and displace Zn but this phenomenon was not associated with oxidative stress mechanism. As observed for MT results, AgNPs or free radicals were potentially chelated to cysteine rich proteins but that was not the predominant pathway compared to dissolved Ag. DA analysis revealed similarities in the biomarker responses between AgNPs and $AgNO_3$ treatment indicating that the toxicity of AgNPs is partly linked to Ag^+. Our results agreed somewhat with those of Gagné et al. (2013) who demonstrated that the effects of AgNPs on MT were partially associated with those of Ag^+ in the digestive gland of the mussel *Elliptio complanata* (Gagné et al., 2013). As mentioned by Jung et al. (2014), AgNPs could be stored in non-specific areas in liver in the cytoplasmic region; this observation would be in agreement with our assumption, unfortunately no hepatic histology was performed in this study.

Decrease in phagocytosis was observed with the AgNPs and was correlated with the increase in COX activity. The decrease in immunoefficiency could provide insight on the size of AgNPs. In fact, when AgNPs exceed the pore size of the wall membrane or cell gap, phagocytosis occurs (Lowry et al., 2012). Another study has demonstrated that the critical cut-off point of endocytosis medium could be 50 nm (Jiang et al., 2008). AgNPs may be internalized by either phagocytosis or endocytosis depending on how AgNPs are presented to cells (aggregates, breakdown products, dissolved Ag).

According to biomarkers results, the two Ag forms induced inflammation processes at the surface of the gills and suppressed phagocytosis. Immune results were different from those observed in our previous study; in Bruneau et al. (2015) we observed no immune disturbance and a slight immunostimulation in fish after 96 h of exposure with 50 μg/L of AgNPs in tap and brown waters respectively. However, $AgNO_3$ induced immunodepression and a significant increase in reduced thiols suggesting that tap water promotes the oxidative stress effects of dissolved form (Bruneau et al., 2015) as observed in this study. Toxic effects of AgNPs to fish were different according to the type of surface water; this conclusion was in agreement with those drawn in Bruneau et al. (2015). In this study, different biochemical pathways for the two Ag forms were observed. Oxidative defense mechanism such as GST and SOD were the main biomarkers that discriminated the $AgNO_3$ from AgNPs treatments. The harmful effect of the ROS could be controlled by the production of proteins that detoxify and repair the damage (Kim and Ryu, 2012). The antioxidant enzymes such as SOD catalase, GST and peroxiredoxins are essential in the maintenance of the organism against oxidative stress. In the present study, the toxic effect of the dissolved form (Ag^+) and produce more oxidative stress than nanoparticulate form. A study of Massarsky et al. (2014b) also found that Ag^+ reduced more the GST activity than AgNPs in trout hepatocytes after an in vitro exposure. A toxicogenomic investigation of Gagné et al. (2012) also found similar results where Ag^+ leads to oxidative stress while AgNP leads to immune effects. Moreover, a decrease in the leucocytes viability was observed with dissolved Ag and not with AgNPs. The mechanistic effects of the AgNPs may be linked to the disaggregation of breakdown of NPs or resulting from the production of free O_2 reactive species. Only, an increase in labile Zn in the gills along with AgNPs was measured, suggesting an increase in the antioxidant defence mechanism, perhaps due to the immediate contact with AgNPs and labile Ag from the AgNPs.

To conclude, both forms of Ag were associated to colloids where $AgNO_3$ were 2.3 times more bioavailable than AgNPs. AgNPs can cause damages to the immune system and inflammation, while dissolved Ag produced more oxidative stress as evidenced by increased GST, MT levels and SOD. It is also suggested that small NPs could be found in the liver of fish in the presence of organic matter from diluted municipal wastewaters. Interestingly, lack of MT induction by the AgNPs suggests also different toxicity pathways than $AgNO_3$.

This study improves our understanding of environmental safety concerns about AgNPs on aquatic organisms. Diluted wastewater, plays a major role in the fate and subsequent bioavailability of the nanomaterials and their transformation products. At expected environmental concentrations of AgNPs, AgNPs should pose a threat to aquatic organisms. Finally, interactions between AgNPs

and other contaminants found in wastewaters should be further considered.

Conflict of interest

The author(s) declare(s) that there is no conflict of interests regarding the publication of this paper.

Acknowledgments

We would like to thank Jean-Philippe Masse from the CM^2 (Centre de Caractérisation Microscopique des Matériaux, École Polytechnique de Montréal, Montréal, Qc) for suppling the TEM. We thank Gwenaël Chamoulaud from NanoQam (Université du Québec à Montréal, Montréal, Qc) for the DLS analyses. We thank the electron microscopy centre team of McGill for TEM gills imagery. We thank Chantale André, Environment Canada, for the elaboration of the MT silver saturation protocol. We thank Carole Fleury from Montreal wastewater treatment plant for providing the samples. Thank to Dr. Richard Cooper for the English writing advices. This work was supported by Environment Canada's Chemicals Management Plan funds.

References

Arora, S., Jain, J., Rajwade, J.M., Paknikar, K.M., 2008. Cellular responses induced by silver nanoparticles: in vitro studies. Toxicol. Lett. 179 (2), 93–100.
Bartneck, M., Keul, H.A., Singh, S., Czaja, K., Bornemann, J., Bockstaller, M., Moeller, M., Zwadlo-Klarwasser, G., Groll, J., 2010. Rapid uptake of gold nanorods by primary human blood phagocytes and immunomodulatory effects of surface chemistry. ACS Nano 4 (6), 3073–3086.
Benn, T.M., Westerhoff, P., 2008. Nanoparticle silver released into water from commercially available sock fabrics. Environ. Sci. Technol. 42 (11), 4133–4139.
Bilberg, K., Malte, H., Wang, T., Baatrup, E., 2010. Silver nanoparticles and silver nitrate cause respiratory stress in Eurasian perch (*Perca fluviatilis*). Aquat. Toxicol. 96 (2), 159–165.
Blaser, S.A., Scheringer, M., MacLeod, M., Hungerbühler, K., 2008. Estimation of cumulative aquatic exposure and risk due to silver: contribution of nano-functionalized plastics and textiles. Sci. Total Environ. 390 (2–3), 396–409.
Bols, N.C., Brubacher, J.L., Ganassin, R.C., Lee, L.E.J., 2001. Ecotoxicology and innate immunity in fish. Dev. Comp. Immunol. 25 (8), 853–873.
Bradford, M.M., 1976. A sensitive method for total protein determination using the principle of protein–dye binding. Anal. Biochem. 72, 249–251.
Braydich-Stolle, L., Hussain, S., Schlager, J.J., Hofmann, M., 2005. In vitro cytotoxicity of nanoparticles in mammalian germline stem cells. Toxicol. Sci. 88 (2), 412–419.
Brousseau, P., Payette, P., Tryphonas, H., Blakley, B., Boermans, H., Flipo, H., Fournier, M. (Eds.), 1998. Manual of Immunological Methods. CRC Press, Boca Raton, Florida.
Bruneau, A., Fortier, M., Gagne, F., Gagnon, C., Turcotte, P., Tayabali, A., Davis, T.L., Auffret, M., Fournier, M., 2013. Size distribution effects of cadmium tellurium quantum dots (CdS/CdTe) immunotoxicity on aquatic organisms. Environ. Sci.: Process. Impacts 15 (3), 596–607.
Bruneau, A., Turcotte, P., Pilote, M., Gagné, F., Gagnon, C., 2015. Fate and immunotoxic effects of silver nanoparticles on rainbow trout in natural waters. J. Nanomed. Nanotechnol. 6 (290).
Bury, Nicolas R., McGeer, J.C., Wood, C.M., 1999. Effects of altering freshwater chemistry on physiological responses of rainbow trout to silver exposure. Environ. Toxicol. Chem. 18 (1), 49–55.
Cumberland, S.A., Lead, J.R., 2009. Particle size distributions of silver nanoparticles at environmentally relevant conditions. J. Chromatogr. A 1216 (52), 9099–9105.
Dobrovolskaia, M.A., McNeil, S.E., 2007. Immunological properties of engineered nanomaterials. Nat. Nanotechnol. 2 (8), 469–478.
Dobrovolskaia, M.A., Aggarwal, P., Hall, J.B., McNeil, S.E., 2008. Preclinical studies to understand nanoparticle interaction with the immune system and its potential effects on nanoparticle biodistribution. Mol. Pharm. 5 (4), 487–495.
Dos Santos, C.A., Seckler, M.M., Ingle, A.P., Gupta, I., Galdiero, S., Galdiero, M., Gade, A., Rai, M., 2014. Silver nanoparticles: therapeutical uses, toxicity, and safety issues. J. Pharm. Sci. 103, 1931–1944.
Erickson, R.J., Brooke, L.T., Kahl, M.D., Venter, F.V., Harting, S.L., Markee, T.P., Spehar, R.L., 1998. Effects of laboratory test conditions on the toxicity of silver to aquatic organisms. Environ. Toxicol. Chem. 17 (4), 572–578.
Ewing, J.F., Janero, D.R., 1995. Microplate superoxide dismutase assay employing a nonenzymatic superoxide generator. Anal. Biochem. 232 (2), 243–248.
Fabrega, J., Fawcett, S.R., Renshaw, J.C., Lead, J.R., 2009. Silver nanoparticle impact on bacterial growth: effect of pH, concentration, and organic matter. Environ. Sci. Technol. 43 (19), 7285–7290.
Fabrega, J., Luoma, S.N., Tyler, C.R., Galloway, T.S., Lead, J.R., 2011. Silver nanoparticles: behaviour and effects in the aquatic environment. Environ. Int. 37 (2), 517–531.
Farkas, J., Christian, P., Gallego-Urrea, J.A., Roos, N., Hassellav, M., Tollefsen, K.E., Thomas, K.V., 2011. Uptake and effects of manufactured silver nanoparticles in rainbow trout (*Oncorhynchus mykiss*) gill cells. Aquat. Toxicol. 101 (1), 117–125.
Farmen, E., Mikkelsen, H.N., Evensen, Ø., Einset, J., Heier, L.S., Rosseland, B.O., Salbu, B., Tollefsen, K.E., Oughton, D.H., 2012. Acute and sub-lethal effects in juvenile Atlantic salmon exposed to low µg/L concentrations of Ag nanoparticles. Aquat. Toxicol. 108, 78–84.
Gagné, F., 2014. Biochemical ecotoxicology. In: Press, A. (Ed.), Principles and Methods. , 1st edition. Academic Press.
Gagné, F., Blaise, C., 1996. Available intracellular Zn as a potential indicator of heavy metal exposure in rainbow trout hepatocytes. Environ. Toxicol. Water Qual. 11, 319–325.
Gagné, F., Auclair, J., Turcotte, P., Fournier, M., Gagnon, C., Sauvé, S., Blaise, C., 2008. Ecotoxicity of CdTe quantum dots to freshwater mussels: impacts on immune system, oxidative stress and genotoxicity. Aquat. Toxicol. 86 (3), 333–340.
Gagné, F., André, C., Skirrow, R., Gélinas, M., Auclair, J., Van Aggelen, G., Turcotte, P., Gagnon, C., 2012. Toxicity of silver nanoparticles to rainbow trout: a toxicogenomic approach. Chemosphere 89 (5), 615–622.
Gagné, F., Auclair, J., Turcotte, P., Gagnon, C., 2013. Sublethal effects of silver nanoparticles and dissolved silver in freshwater mussels. J. Toxicol. Environ. Health A 76 (8), 479–490.
Gagnon, Christian, Gagné, François, Turcotte, Patrice, Saulnier, Isabelle, Blaise, Christian, Salazar, Michael H., Salazar, Sandra M., 2006. Exposure of caged mussels to metals in a primary-treated municipal wastewater plume. Chemosphere 62 (6), 998–1010.
Gomes, T., Pereira, C.G., Cardoso, C., Sousa, V.S., Teixeira, M.R., Pinheiro, J.P., Bebianno, M.J., 2014. Effects of silver nanoparticles exposure in the mussel *Mytilus galloprovincialis*. Mar. Environ. Res. 101, 208–214.
Gottschalk, F., Sonderer, T., Scholz, R.W., Nowack, B., 2009. Modeled environmental concentrations of engineered nanomaterials (TiO_2, ZnO, Ag, CNT, fullerenes) for different regions. Environ. Sci. Technol. 43 (24), 9216–9222.
Griffitt, R.J., Luo, J., Gao, J., Bonzongo, J.C., Barber, D.S., 2008. Effects of particle composition and species on toxicity of metallic nanomaterials in aquatic organisms. Environ. Toxicol. Chem. 27 (9), 1972–1978.
Griffitt, R.J., Hyndman, K., Denslow, N.D., Barber, D.S., 2009. Comparison of molecular and histological changes in zebrafish gills exposed to metallic nanoparticles. Toxicol. Sci. 107 (2), 404–415.
Griffitt, R.J., Lavelle, C.M., Kane, A.S., Denslow, N.D., Barber, D.S., 2013. Chronic nanoparticulate silver exposure results in tissue accumulation and transcriptomic changes in zebrafish. Aquat. Toxicol. 130–131, 192–200.
Handy, R.D., Henry, T.B., Scown, T.M., Johnston, B.D., Tyler, C.R., 2008. Manufactured nanoparticles: their uptake and effects on fish—a mechanistic analysis. Ecotoxicology 17 (5), 396–409.
Jiang, W., Kim, B.Y.S., Rutka, J.T., Chan, W.C.W., 2008. Nanoparticle-mediated cellular response is size-dependent. Nat. Nanotechnol. 3 (3), 145–150.
Jovanović, B., Palić, D., 2012. Immunotoxicology of non-functionalized engineered nanoparticles in aquatic organisms with special emphasis on fish—review of current knowledge, gap identification, and call for further research. Aquat. Toxicol. 118, 141–151.
Jung, Y., Kim, K., Kim, J.Y., Yang, S., Lee, B., Kim, S.D., 2014. Bioconcentration and distribution of silver nanoparticles in Japanese medaka (*Oryzias latipes*). J. Hazard. Mater. 267, 206–213.
Kaegi, R., Voegelin, A., Sinnet, B., Zuleeg, S., Hagendorfer, H., Burkhardt, M., Siegrist, H., 2011. Behavior of metallic silver nanoparticles in a pilot wastewater treatment plant. Environ. Sci. Technol. 45 (9), 3902–3908.
Kim, S., Ryu, D.Y., 2012. Silver nanoparticle-induced oxidative stress, genotoxicity and apoptosis in cultured cells and animal tissues. J. Appl. Toxicol. 33 (2), 78–89.
King, S.M., Jarvie, H.P., 2012. Exploring how organic matter controls structural transformations in natural aquatic nanocolloidal dispersions. Environ. Sci. Technol. 46 (13), 6959–6967.
Li, L., Hartmann, Georg, Döblinger, Markus, Schuster, Michael, 2013. Quantification of nanoscale silver particles removal and release from municipal wastewater treatment plants in Germany. Environ. Sci. Technol. 47 (13), 7317–7323.
Limbach, L.K., Bereiter, R., Müller, E., Krebs, R., Gälli, R., Stark, W.J., 2008. Removal of oxide nanoparticles in a model wastewater treatment plant: influence of agglomeration and surfactants on clearing efficiency. Environ. Sci. Technol. 42 (15), 5828–5833.
Lowry, G.V., Gregory, K.B., Apte, S.C., Lead, J.R., 2012. Transformations of nanomaterials in the environment. Environ. Sci. Technol. 46 (13), 6893–6899.
Massarsky, A., Trudeau, V.L., Moon, T.W., 2014a. Predicting the environmental impact of nanosilver. Environ. Toxicol. Pharmacol. 38 (3), 861–873.
Massarsky, A., Abraham, R., Nguyen, K.C., Rippstein, P., Tayabali, A.F., Trudeau, V.L., Moon, T.W., 2014b. Nanosilver cytotoxicity in rainbow trout (*Oncorhynchus mykiss*) erythrocytes and hepatocytes. Biochem. Physiol.—C Toxicol. Pharmacol. 159 (1), 10–21.
Morones, J.R., Elechiguerra, J.L., Camacho, A., Holt, K., Kouri, J.B., Ramirez, J.T., Yacaman, M.J., 2005. The bactericidal effect of silver nanoparticles. Nanotechnology 16 (10), 2346–2353.

NRC, 2012. A Research Strategy for Environmental, Health, and Safety Aspects of Engineered Nanomaterials. The National Academies Press, Washington, DC.
Olive, P.L., 1988. DNA precipitation assay: a rapid and simple method for detecting DNA damage in mammalian cells. Environ. Mol. Mutagen. 11 (4), 487–495.
Osborne, O.J., Johnston, B.D., Moger, J., Balousha, M., Lead, J.R., Kudoh, T., Tyler, C.R., 2013. Effects of particle size and coating on nanoscale Ag and TiO_2 exposure in zebrafish (*Danio rerio*) embryos. Nanotoxicology 7 (8), 1315–1324.
Philippe, A., Schaumann, G.E., 2014. Interactions of dissolved organic matter with natural and engineered inorganic colloids: a review. Environ. Sci. Technol. 48 (16), 8946–8962.
Project on Emerging Nanotechnologies, (cited 26.01.16) http://www.nanotechproject.org/cpi.
Ribeiro, F., Gallego-Urrea, J.A., Jurkschat, K., Crossley, A., Hassellöv, M., Taylor, C., Soares, A.M.V.M., Loureiro, S., 2014. Silver nanoparticles and silver nitrate induce high toxicity to *Pseudokirchneriella subcapitata*: *Daphnia magnaDaphnia magna* and *Danio rerio*. Sci. Total Environ. 466–467, 232–241.
Scheuhammer, A.M., Cherian, M.G., 1986. Quantification of metallothioneins by a silver-saturation method. Toxicol. Appl. Pharmacol. 82 (3), 417–425.
Scown, T.M., Santos, E.M., Johnston, B.D., Gaiser, B., Baalousha, M., Mitov, S., Lead, J.R., Stone, V., Fernandes, T.F., Jepson, M., 2010. Effects of aqueous exposure to silver nanoparticles of different sizes in rainbow trout. Toxicol. Sci. 115 (2), 521–534.
Siripattanakul-Ratpukdi, S., Fürhacker, M., 2014. Review: issues of silver nanoparticles in engineered environmental treatment systems. Water Air Soil Pollut. 225 (4), 1–18.
Unrine, J.M., Colman, B.P., Bone, A.J., Gondikas, A.P., Matson, C.W., 2012. Biotic and abiotic interactions in aquatic microcosms determine fate and toxicity of Ag nanoparticles. Part 1: aggregation and dissolution. Environ. Sci. Technol. 46 (13), 6915–6924.
Walker, M., Parsons, D., 2012. The biological fate of silver ions following the use of silver-containing wound care products—a review. Int. Wound J. 11 (5), 496–504, http://dx.doi.org/10.1111/j.1742-481X.2012.01115.x, October 2014.
Welsh, P.G., Skidmore, J.F., Spry, D.J., Dixon, D.G., Hodson, P.V., Hutchinson, N.J., Hickie, B.E., 1993. Effect of pH and dissolved organic carbon on the toxicity of copper to larval fathead minnow (*Pimephales promelas*) in natural lake waters of low alkalinity. Can. J. Fish. Aquat. Sci. 50 (7), 1356–1362.
Wills, E.D., 1987. Evaluation of lipid peroxidation in lipids and biological membranes. In: Snell, K., Mullock, B. (Eds.), Biochemical Toxicology: A Practical Approach. IRL Press, Washington, DC.
Zahr, A.S., Davis, C.A., Pishko, M.V., 2006. Macrophage uptake of core-shell nanoparticles surface modified with poly(ethylene glycol). Langmuir 22 (19), 8178–8185.
Zapata, A., 1979. Ultrastructural study of the teleost fish kidney. Dev. Comp. Immunol. 3, 55–65.